A wearable multi-channel fNIRS system for brain imaging in freely moving subjects

Sophie K. Piper [a,*], Arne Krueger [a], Stefan P. Koch [a], Jan Mehnert [a,b], Christina Habermehl [a], Jens Steinbrink [a,b], Hellmuth Obrig [c,d], Christoph H. Schmitz [a,e,1]

[a] Charité University Medicine Berlin, Department of Neurology, Charitéplatz 1, 10117 Berlin, Germany
[b] Charité University Medicine Berlin, Center for Stroke Research Berlin, Charitéplatz 1, 10117 Berlin, Germany
[c] Max Planck Institute for Human Cognitive and Brain Sciences, Stephanstr. 1a, 04103 Leipzig, Germany
[d] Clinic for Cognitive Neurology, University Hospital Leipzig, Liebigstr. 16, 04103 Leipzig, Germany
[e] NIRx Medizintechnik GmbH, Baumbachstr. 17, 13189 Berlin, Germany

ARTICLE INFO

ABSTRACT

Functional near infrared spectroscopy (fNIRS) is a versatile neuroimaging tool with an increasing acceptance in the neuroimaging community. While often lauded for its portability, most of the fNIRS setups employed in neuroscientific research still impose usage in a laboratory environment. We present a wearable, multi-channel fNIRS imaging system for functional brain imaging in unrestrained settings. The system operates without optical fiber bundles, using eight dual wavelength light emitting diodes and eight electro-optical sensors, which can be placed freely on the subject's head for direct illumination and detection. Its performance is tested on N = 8 subjects in a motor execution paradigm performed under three different exercising conditions: (i) during outdoor bicycle riding, (ii) while pedaling on a stationary training bicycle, and (iii) sitting still on the training bicycle. Following left hand gripping, we observe a significant decrease in the deoxyhemoglobin concentration over the contralateral motor cortex in all three conditions. A significant task-related ΔHbO_2 increase was seen for the non-pedaling condition. Although the gross movements involved in pedaling and steering a bike induced more motion artifacts than carrying out the same task while sitting still, we found no significant differences in the shape or amplitude of the HbR time courses for outdoor or indoor cycling and sitting still. We demonstrate the general feasibility of using wearable multi-channel NIRS during strenuous exercise in natural, unrestrained settings and discuss the origins and effects of data artifacts. We provide quantitative guidelines for taking condition-dependent signal quality into account to allow the comparison of data across various levels of physical exercise. To the best of our knowledge, this is the first demonstration of functional NIRS brain imaging during an outdoor activity in a real life situation in humans.

© 2013 Elsevier Inc. All rights reserved.

Introduction

Functional near infrared spectroscopy (fNIRS) is a versatile neuroimaging tool with an increasing acceptance in the neuroimaging community (Ferrari and Quaresima, 2012; Huppert et al., 2009). It is an effective and non-invasive tool for monitoring oxygenation and cerebral hemodynamics (Boas et al., 2004; Villringer and Chance, 1997) showing good agreement with simultaneously acquired fMRI measurements (Eggebrecht et al., 2012; Hoge et al., 2005; Huppert et al., 2006; Kleinschmidt et al., 1996; Steinbrink et al., 2006; Strangman et al., 2002). It has been promoted for its i) non-invasive, non-ionizing nature, ii) bed-side applicability (Obrig and Villringer, 2003; Steinkellner et al., 2010; Tobias, 2006; Toet and Lemmers, 2009), iii) relatively low costs,

iv) ease of integration with other modalities such as electro encephalography (EEG) (Fazli et al., 2012; Lareau et al., 2011; Moosmann et al., 2003; Obrig et al., 2002; Wallois et al., 2012) or functional magnetic resonance imaging (fMRI)(Cooper et al., 2012; Mehagnoul-Schipper et al., 2002; Strangman et al., 2002), and for its v) portability (Atsumori et al., 2007; Bozkurt et al., 2005; Kiguchi et al., 2012; Muehlemann et al., 2008; Vaithianathan, 2004).

While today there is good evidence for the aforementioned advantages, most of the NIRS setups employed in neuroscientific research still offer a spatially restrained setting. Typically, rather bulky and not very flexible fiber-optic cables tie the subjects to a more or less stationary instrument (Eggebrecht et al., 2012; Habermehl et al., 2012a, 2012c; Holtzer et al., 2011; Koch et al., 2012; Kurz et al., 2012; Shalinsky et al., 2009). Furthermore, size and weight of fiber-optic cables are prone to inducing motion artifacts by dislocating the probes. While restrained settings with a portable but stationary instrument might be well feasible for bedside monitoring, they hamper imaging in a more natural

---

* Corresponding author. Fax: +49 30 450 560 936.
  E-mail address: Sophie.Piper@charite.de (S.K. Piper).
[1] Author CS is an employee of NIRx Medizintechnik GmbH, Berlin.

environment, for example outside the laboratory, during sports or physical therapy, when social interactions between subjects are required, or when imaging children.

Developments towards miniaturized probe arrays, portable and even wireless instruments have been reported for over ten years now; however, usually at the cost of a low number of measurement channels, the restriction to specific portions of the head, or the focus on a specific age group (Atsumori et al., 2007; Bozkurt et al., 2005; Hoshi and Chen, 2002; Muehlemann et al., 2008; Sagara et al., 2009; Yurtsever et al., 2003). There is a recent trend in diffuse optical brain imaging towards higher channel counts to either allow for high-density tomographic imaging (Dehghani et al., 2009; Eggebrecht et al., 2012; Habermehl et al., 2012a; White and Culver, 2010) and/or to provide greater coverage of one or multiple portions of the head (Mehnert et al., in press).

Following this tendency, there is great interest in portable NIRS systems with an increasing number of measurement channels (Atsumori et al., 2009; Kiguchi et al., 2012; Vaithianathan, 2004) and possibly hybrid portable NIRS-EEG systems (Lareau et al., 2011).

Here we present a miniaturized, portable diffuse optical NIR imaging system that allows multi-channel brain imaging in freely moving subjects and lends itself readily to general-purpose large-area imaging of brain activity (Krueger et al., 2012). The performance of the instrument is tested on N = 8 subjects in a hand gripping motor paradigm on a bicycle performed during three conditions: (i) outdoor bicycle riding, (ii) indoor pedaling on a training bicycle and (iii) sitting still. To the best of our knowledge, this is the first demonstration of functional NIRS brain imaging during an outdoor activity in a real life environment.

Material and methods

Instrumentation

The wearable NIRS instrument utilizes eight dual-wavelength light emitting diodes (LED) for direct skin illumination. We employ time-multiplexing of the source positions with simultaneous frequency-encoded dual-wavelength illumination. Each LED contains two emitters at 760 nm and 850 nm with a spectral half-width of 25 nm and 30 nm, respectively. The emitters are intensity-modulated at 1.0 and 1.1 kHz, and each radiate approximately 10 mW of average optical power during their 'on' state. The LED has a 3-mm diameter clear plastic dome package which is brought into direct contact with the skin (L760/850-36 by Epitex Inc., Japan). The LED is mounted inside a custom-made plastic optode housing which is placed in the head cap (see Fig. 1).

Optical detection is performed with eight photo-electrical receivers, each of which contains a Silicon photodiode (SiPD, BPW34, Siemens, Germany) followed by a transimpedance amplifier with a fixed 10-MΩ feedback resistor. The circuitry is housed in the internally shielded optode enclosure, which can be inserted into the head cap (see Figs. 1 and 2). A 12-mm segment of a plastic optical fiber guide (outside diameter: 3 mm, numerical aperture: 0.50, type NT53-833 by Edmund Optics, Barrington, NJ, USA) serves to couple light from the skin to the Si-PD sensitive area. To maximize the signal-to-noise ratio, the electrical signal from each detector is further amplified within the main instrument by programmable gain amplifiers, whose gain is switched synchronously with the source positions (Schmitz et al., 2002).

The cables connecting to the emitters and receivers were selected in order to maximize flexibility and robustness and to minimize weight and bulk. We employed a highly flexible, braid-shielded, three-wire (each 0.014 mm^2) cable with an outer Polyurethane sheath (outer cable diameter = 1.4 mm). Identical cables were used for sources and detectors. Near the head the individual source and detector cables are grouped and connected to two flat ribbon cables which run to the imager. The interface between the two cable types is formed by a small plastic enclosure which only contains passive connections, and which serves to provide stability and strain relief (gray boxes attached to the head cap in Fig. 2). The system puts an end to optical fiber bundles, thereby avoiding the optical signal losses associated with fiber-optics, as well as their bulk and weight. This lightens the probe weight on the subject's head considerably and makes the setup more stable against motion artifacts. Furthermore, avoiding fiber-optics and opto-mechanical coupling components reduces the overall instrument size, weight, and cost.

The main instrument contains a data acquisition board (DAQ, NI-USB 6216, National Instruments, Austin, TX, USA (NI)) and a single 160 mm × 100 mm custom-designed printed circuit board, both placed in a 103 mm × 43 mm × 167 mm aluminum enclosure. Data transfer and power supply are realized though two USB 2.0 connections to a small notebook computer running a graphical user interface for instrument control, data display, and storage, programmed in LabVIEW 2011 (National Instruments, Austin, TX, USA). The overall sampling rate is 6.25 Hz. The instrument and controlling notebook computer can be worn in a backpack and allow continuous measurements for about 2 h without recharging (Fig. 2). The system was later upgraded with an internal rechargeable battery which reduces the number of necessary USB connections to a single USB connection and increases the measurement time to eight hours (not accounting for notebook PC battery life). The system can broadcast measured data in real time over a wireless local area network which allows high band width and quite large operating distances (this feature was not used in the current study).

Sources and detectors can be arranged in any application-specific source-detector-geometry provided a detector is within the ~30 mm measuring range of a source.

Experimental design

We measured eight healthy subjects (six male, two female, age 24–43) performing ten repetitions of self-paced left hand gripping (20 s gripping followed by 40 s of rest) under three different experimental conditions. All of these were performed sitting on a bicycle and consisted of (i) outdoor bicycle riding, (ii) indoor pedaling on a training bicycle, and (iii) sitting still. The hand-gripping task serves methodological demonstration similar to (Muehlemann et al., 2008). Generally, a block paradigm with a 20 to 30 s task period is commonly used in motor studies with NIRS (Atsumori et al., 2010; Franceschini et al., 2003; Habermehl et al., 2012a; Koenraadt et al., 2012; Kurz et al., 2012). A rather long resting period of 40 s was
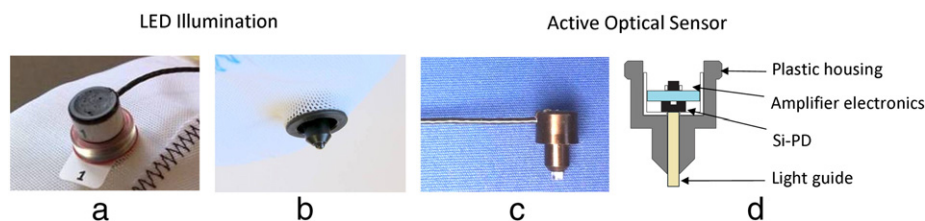

Fig. 1. LED source and electro-optical sensor developed for the wearable miniaturized NIRS system. Left: dual wavelength LED source in customized enclosure on fabric cap from (a) above and (b) below. Right: (c) photograph and (d) schematic of the detector probe. A plastic optical fiber light guide couples the light re-emitted from the head to a Silicon photo diode (Si-PD) with amplifier.
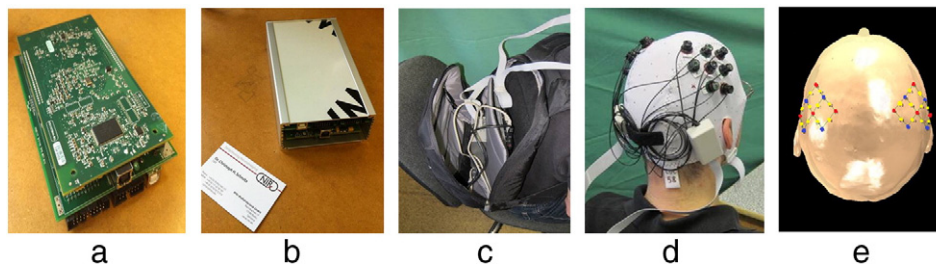
Fig. 2. The wearable miniaturized NIRS System: (a) DAQ board and main board of the disassembled prototype, (b) aluminum enclosure of the main instrument with a size of 103 mm × 43 mm × 167 mm, (c) NIRS imager and control laptop stowed in a backpack, (d) dual 4-source/4-detector setup over left and right motor cortex as used for the bicycle experiment, and (e), position of NIRS measurement channels on the head surface, red: sources, blue: detectors, yellow: measurement positions.

chosen to avoid non-linear effects of the hemodynamic refractory period (Cannestra et al., 1998), to assure the hemodynamic response's return to baseline activity, and to mitigate any effects of anticipation of the next task period (Obrig et al., 1997). The three different conditions were recorded in a randomized order. For conditions (i) and (ii) an initial 3 min pedaling period was allowed to settle the cardiac rate. During outdoor bicycling, subjects followed a pre-described, straight and level bike lane at a brisk pace (15–20 km/h). Auditory commands 'start' and 'stop' were issued by in-ear headphones to indicate the onset and cessation of left-hand motion on a dummy hand brake lever which was mounted to the handlebars and did not cause the bicycle to brake. Time-stamped markers were recorded synchronously with these events. Subjects were asked to use the dummy handbrake lever at a constant pace of about 1 Hz and with a constant gripping strength in all conditions. For safety reasons, the cyclist was accompanied by another person on a second bike throughout the duration of the experiment. All subjects used the same bicycle for all three conditions.

During the pedaling tasks, the constant lower limb activity can be regarded as background activity, which may cause a constant shift of the activation baseline in conditions (i) and (ii). In contrast, the periodic hand movement causes well-defined activation modulations with respect to the baseline, so that the event-related analysis of these changes allows the exploration of the functional cortical activation in 'increasingly ecological' situations. Performing the hand-gripping paradigm while sitting still on the bicycle serves as an independent control condition, that is to say, measuring under stationary and laboratory conditions at the lowest possible level of background activity.

To cover the primary motor areas of both hemispheres, optodes were arranged in two groups (four sources and four detectors each) clustered around positions C3 and C4 of the extended international EEG 10–20 system. This resulted in a total of 20 NIRS measurement channels for each of the two wavelengths. The inter-optode distance between neighboring source-detector-pairs was 25 ± 3 mm (mean ± maximum deviation). The cap and probe placement was performed indoors, with the subject sitting comfortably. After calibration of the detector gains to optimize the signal-to-noise ratios, and after assuring good tissue contact of all probes, the laptop and NIRS device were stowed in a backpack, which was then donned by the subject. The added time to prepare the subject for the mobile experiment added only a few minutes to the usual NIRS setup time. A bandage and a dark woolen cap worn over the optical probes served to improve probe-tissue-contact, shield ambient light and to provide stabilization against motion artifacts. None of the subjects reported discomfort.

Data processing and analysis

All data analysis and display were performed using customized routines in MATLAB (The MathWorks, Inc., Natick, MA, USA). Relative changes in oxy- (HbO_2) and deoxygenated hemoglobin (HbR) for each measurement position were calculated from the raw light intensity data by applying the modified Beer–Lambert law (Kocsis et al., 2006).

A differential path length factor (DPF) of 5.98 for 850 nm and 7.15 for 760 nm as published by Essenpreis (Essenpreis et al., 1993) was applied. The corresponding molar extinction coefficients ε for HbO_2 and HbR, ε_{850nm} = [1097.0 781.0] cm^{-1}/M and ε_{760nm} = [645.5 1669.0] cm^{-1}/M, were compiled by Scott Prahl (Prahl and O.M.L.C., 2006) using data from W. B. Gratzer, Med. Res. Council Labs, Holly Hill, London and N. Kollias, Wellman Laboratories, Harvard Medical School, Boston.

Time courses of relative hemoglobin concentrations changes were bandpass-filtered (first order Butterworth filter, $f_{cutoff,\ low}$ = 0.011 Hz, $f_{cutoff,\ hi}$ = 0.2 Hz) to reject heartbeat, breathing and drifts. Furthermore, we applied a 0.09–0.11 Hz bandstop filter to suppress physiological systemic oscillations dominating the HbO_2 time courses. From the continuously acquired data we extracted single trials from −10 s to 50 s relative to the start of each hand gripping period. As the hemodynamic baseline for each trial we defined the 10 s period preceding each activation onset.

To estimate the signal-to-noise performance of a data channel, the relative coefficient of variation (CV, in %) was calculated for the unfiltered raw data (intensity changes), which is a common procedure for multi-channel NIRS measurements (Schmitz et al., 2005; Schneider et al., 2011):

$$CV = \frac{\sigma}{\mu} \cdot 100\%$$

Here, σ is the temporal standard deviation for a data channel, and μ is the corresponding mean value. Possible sources of reduced signal-to-noise ratio (=increased CV) due to physical exercise include physical artifacts such as motion-induced instabilities of the coupling efficiency at the tissue-optical interfaces as well as physiological artifacts such as blood-pressure induced hemodynamics.

Two measures were derived: CV_{chan} was computed over the entire duration of the experiment (10 min) to compare the data quality between channels, and CV_{trial} was obtained for 60-s intervals of the individual trials to estimate the trial-to-trial variation.

Measurement channels with a CV_{chan} exceeding 15% were rejected, and of the remaining channels only trials with a CV_{trial} of less than 5% in both wavelengths were kept for further processing and analysis. Fig. 3 shows the effect of our exclusion criteria on the hemodynamic signals for some exemplary data sets and Table 1 gives an overview of channel and trial rejection rates in each condition. Inline Supplementary Figs. S1 and S2 show histograms of the calculated CV values to indicate the quality of the acquired data.

Inline Supplementary Figs. S1 and S2 can be found online at http://dx.doi.org/10.1016/j.neuroimage.2013.06.062.

For a valid statistical comparison of the activation maps across the three conditions we considered only those channels which met the above defined quality criteria in all three conditions (see Fig. 3). The remaining trials were averaged to get mean relative hemoglobin concentration changes for each subject, measurement channel, and experimental condition.

Brain activation was identified as a significant increase in ΔHbO_2 or a significant decrease in ΔHbR by calculating the relative difference in the temporal mean of the averaged ΔHbO_2 and ΔHbR levels between 8 s and 20 s after hand-gripping onset with respect to the average baseline, similar to (Kiguchi et al., 2012; Koenraadt et al., 2012). These values were tested against zero with a one-sided *t*-test within each channel. To account for multiple comparisons, *p*-values were Bonferroni-corrected, setting the significance level to $p = 0.05/20 = 0.0025$. The *t*-values of significant ΔHbR channels were color-coded and spatially projected onto the gray matter surface of a normalized structural MR scan acquired from one volunteer (male, age 41) and affine-transformed to the Montreal Institute of Neuroimaging's (MNI) standard brain model (Brett et al., 2002). The spatial co-registration of NIRS probes relies on relative distances to standard electrodes of the 10–20 EEG electrode system.

For the channels reaching significance we used a balanced one-way ANOVA on the data between 8 s and 20 s after activation onset to test for differences between the three conditions. The null hypothesis tested herein was that the samples in all three conditions are from populations with the same mean value. The significance level *p* to reject the null hypothesis was $p < 0.05$.

Group averages were calculated for all included data channels and each condition, respectively. Furthermore, group averaged time courses in significant data channels are displayed with standard error of mean (SEM). The standard deviation, which reflects variance in individual measurements, can be calculated as $\sqrt{N} \cdot SEM$ for each time point, with N being the number of subjects.

Results

The newly developed wearable multi-channel NIRS system ran without technical problems for all eight subjects throughout all experimental conditions.

Table 1 summarizes the number of channels and trials rejected for the different conditions from our analysis, based on our noise criteria of $CV_{chan} > 15\%$ and $CV_{trial} > 5\%$.

On average, 7 of the 20 measurement channels had to be excluded in the outdoor bicycling condition, whereas less than two channels had to be excluded under laboratory conditions on a stationary bike. This suggests that mechanical motion artifacts, which were greatest during actual bicycling, were the primary cause of channel dropouts. To account for this dropout rate, about 30–40% more subjects would be required in the outdoor condition compared to a controlled laboratory setting.

Fig. 4 shows the group averaged oxygenation changes and brain activation maps for all three conditions. The hemodynamic signals of the significant channel show the prototypical increase in ΔHbO_2 and decrease in ΔHbR in response to neuronal activation throughout all conditions. The shown SEM levels suggest a greater hemodynamic
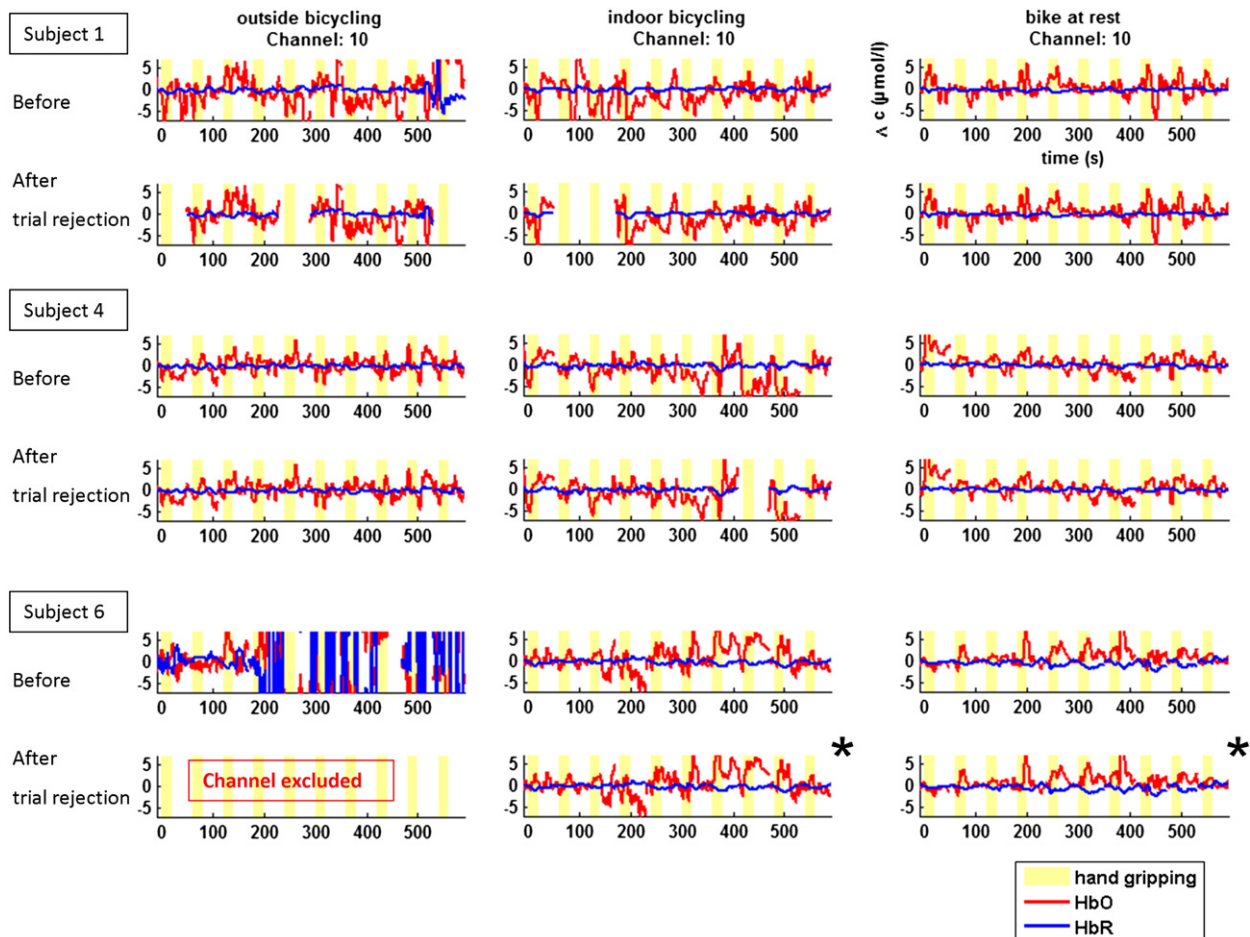

Fig. 3. Continuous time courses of relative HbO_2 and HbR changes before and after artifact rejection while outdoor bicycling (left), stationary bicycling (middle), and sitting still (right) for three representative subjects. Each trial is baseline corrected to $(-10–0)$ s before each hand gripping onset (yellow bars: 20-s hand gripping activation periods). Trials and channels exceeding our noise limits were removed from the data time series and excluded from further analysis. For a valid statistical comparison across the three conditions, we considered only those channels which met the defined quality criteria in all three conditions within a subject. As a result, data denoted by (*) were also excluded from the further analysis. Oscillations of physiological origin are generally more pronounced in the ΔHbO_2 data compared to the ΔHbR Signals. Nevertheless, the prototypical neuro-activation response is seen in many instances, even without event-related averaging.

Table 1

Overview of channel and trial rejection rates in each condition based on our coefficient of variation criteria ($CV_{chan} > 15\%$, $CV_{trial} > 5\%$). Shown in parenthesis are the corresponding standard deviation (SD) values; numbers in brackets indicate extreme values [minimum–maximum].

	Outdoor bicycle riding	Indoor pedaling on stationary bike	Indoor sitting on stationary bike
Rejected channels/subject (SD)	35 (35) %	7.5 (10) %	5 (5) %
Fewest/most channels rejected: [Min–Max]	[0–20]	[0–7]	[0–4]
Rejected trials/all trials, all included channels, all subjects (SD)	4 (6) %	2.5 (3) %	2.5 (2) %
Fewest/most trials rejected: [Min–Max]	[0–17]%	[0–9]%	[0–5]%

variability in the HbO_2 signal especially during the biking activity. Interestingly, the HbR signals are much less affected by the physical activity and are reproducible over different conditions (see the discussion for more detail).

A focal hemodynamic response to left hand activation is revealed in all three conditions by a significant mean relative decrease in HbR ($p < 0.0025$) over the contralateral motor cortex, fronto-medial from standard EEG electrode position C4 (measurement channel 10). The mean decrease in HbR was (0.4 ± 0.2) µmol/l for outdoor bicycle riding, (0.5 ± 0.2) µmol/l for stationary pedaling, and (0.3 ± 0.2) µmol/l for sitting still (mean $\pm$ standard deviation). A significant ΔHbO_2 response was only observed in the non-pedaling condition. This however, was not focal but instead spread out over both hemispheres (12 of the 20 channels, data not shown).

Fig. 5 shows the topographic arrangement of the group-averaged ΔHbR time courses for all three conditions in all measurement channels as well as a magnified view of the significant channel no. 10. Indicated for each channel is the number of subjects that were included in the average, that is to say, the number of subjects for which $CV_{chan} < 15\%$.

For the activation channel, the mean ΔHbR time courses during left hand gripping show no significant differences between the three conditions ($p > 0.05$). The functional cerebral activation due to the pedaling action in conditions (i) and (ii), therefore, plays a minor role compared to the hand gripping related oxygenation changes. The corresponding mean ΔHbO_2 time courses show a stimulus-related global increase of oxygenation in all channels for all conditions. However, these changes

are only significant for the resting condition (see Inline Supplementary Fig. S3).

Inline Supplementary Fig. S3 can be found online at http://dx.doi.org/10.1016/j.neuroimage.2013.06.062.

Discussion

We demonstrated the performance of a wearable, multi-channel diffuse optical NIR imaging system in a hand gripping motor paradigm while (i) outdoor bicycle riding, (ii) indoor bicycle pedaling on a training bicycle and (iii) rest.

Neuronal activation from left hand gripping was indicated by a focal HbR decrease over the contralateral motor cortex. Whereas the raw signals show a clear influence on the presence and severity of physical exercise, the measured HbR activation levels did not differ for the three experimental conditions. The observed decrease in HbR following neuro-activation is well described in the literature on a fundamental physiological neuro-vascular coupling level and has been validated in animal experiments, and in numerous human NIRS studies (Hoge et al., 2005; Huppert et al., 2006; Kleinschmidt et al., 1996; Strangman et al., 2002). While there are fNIRS studies primarily focusing on HbO_2 measurements (Atsumori et al., 2010; Holtzer et al., 2011; Kurz et al., 2012; Suzuki et al., 2004, 2008) due to their improved signal-to-noise ratio relative to the HbR measurements and their reduced vulnerability to cross talk (Boas et al., 2004; Leff et al., 2011; Strangman et al., 2003), our results are in line with the hypothesis that the HbR signal is less influenced
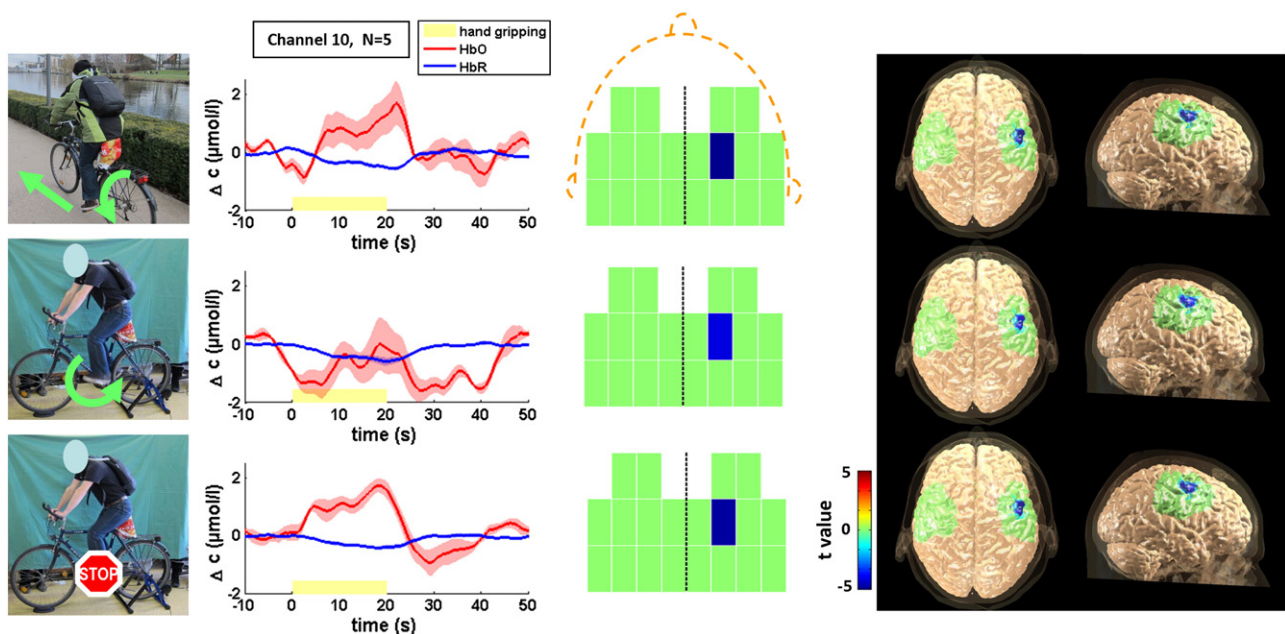

Fig. 4. Experimental conditions (left column), average reconstructed oxygenation changes with SEM (second column) and topographic mapping of all significant HbR NIRS channels (two right columns) during left hand gripping for each experimental condition. Left column, top to bottom: outdoor bicycle riding, stationary bike pedaling, resting on a stationary bike. Second column: Event-related average of the relative HbO_2 (red) and HbR (blue) concentration changes in the significant HbR channel with standard error of the mean during the hand-gripping motor task (yellow: 20-s hand gripping period). Third column: topographic maps of the significant ΔHbR channels, with color-coded t-value after Bonferroni-Correction for multiple comparison ($p < 0.0025$). Right column: projection of the measured HbR concentration response to hand gripping onto a representative cortical surface map in MNI space. The field of view probed by the NIRS array corresponds to the green areas.

by global hemodynamics such as motion induced changes in the cardiac pulsation, systemic blood pressure, respiration, vasomotor oscillations, or Mayer wave fluctuations (Gregg et al., 2010; Habermehl et al., 2012b; Huppert et al., 2009; Kirilina et al., 2012; Obrig et al., 2000; Saager and Berger, 2008; Zhang et al., 2005, 2009). These pulsatile parts are predominantly present in the arterial compartments that are typically more than 95% oxygenated and therefore appear mostly in the HbO_2 signal (Huppert et al., 2009). In our system the 760 nm and 850 nm excitation wavelengths were chosen to optimize the SNR issue in the HbR measurements (Sato et al., 2004). We therefore take the significant focal HbR decrease to be a reliable indicator for a task-related neuronal activation for the experiment presented here.

The group average also suggested an event-related global HbO_2 increase. However, for the included number of subjects and trials this finding only reached the significance level in the resting condition because of the greater signal variability of the HbO_2 signals compared to HbR with physical exercise (Kirilina et al., 2012). The SEM of the group average HbO_2 time courses exceeds that of the HbR in all conditions, but is largest in the two pedaling experiments. A greater hemodynamic variability in the HbO_2 signal especially during bicycling is expected because of greater blood pressure and heart rate variability during exercise. This finding supports the notion that, after rejecting physical artifacts in the raw data based on a simple stability criterion, the HbO_2 signal is much more sensitive to the physiological artifacts of the cardiac modulations caused by strenuous physical exercise (Boas et al., 2004; Huppert et al., 2009; Kirilina et al., 2012; Leff et al., 2011; Zhang et al., 2005). Moreover, this implies that it is not the physical measurement stability artifacts but rather the physiological extra-cerebral noise which is the limiting factor for functional NIRS studies under exercise.

There are instrumental and/or signal analysis schemes to reduce the interference from global hemodynamics, such as the use of multi-distance measurements for nearest neighbor regression (Gregg et al., 2010; Saager and Berger, 2008), principal component analysis to identify task-related signal components (Kurz et al., 2012) or artifact (Boas et al., 2004; Zhang et al., 2005), general linear model approaches (Kirilina et al., 2012) or adaptive filtering (Zhang et al., 2009). However, no common standard has yet been established in dealing with extraneous biological noise, and evaluating these approaches is beyond the scope of our manuscript. Furthermore, we show that a stable hemodynamic response can be achieved in a rather limited number of subjects and trials for freely moving humans by employing a simple rejection of mechanical motion artifacts and analysis on the HbR signal.

For the number of subjects and trials evaluated in this study, we found no significant difference in the measured motor-activation for pedaling vs. non-pedaling tasks, or between stationary vs. actual bicycling. We explain this observation to be a result of the comparatively week and constant NIRS signal caused by the continuous activities of the lower extremities, the effect of which is largely removed by the task-related block average. This is in line with the observations of Atsumori et al. (2010) who find the impact of continuous walking on the task-induced oxygenation changes to be small. Also, any physiological noise potentially caused by additional motions of actual or stationary bicycle riding (leg movement, steering, head movements, etc.) are uncorrelated to the task timing and do not present a cause of major noise in the task-related signals.

NIRS has proven to be a valuable research tool in many areas despite its known technical limitations related to penetration depth, spatial resolution, and interference by contact based measurement (Boas et al., 2004; Leff et al., 2011). While the penetration depth is limited by physical principles which may not be overcome, NIRS resolution can be improved to the sub-centimeter range by dense spatial sampling (Eggebrecht et al., 2012; Habermehl et al., 2012a, 2012c). The third concern of NIRS, i.e. optical contact induced interferences and tethering of the subject can be greatly alleviated by miniaturized wearable probes such as demonstrated in the present work.

Portable and miniaturized NIRS systems open new perspectives for the study of sensory or cognitive paradigms in realistic environments. Similar to wireless EEG systems which proved stable in 'real world' measurements (Gevins et al., 2012), being able to measure cerebral function outside the laboratory gives room for new desirable applications. Muehlemann et al. (2013) used their in-house built wireless miniaturized NIRS system to study the effect of sudden depressurization on pilots at cruising altitude. Other examples where wearable NIRS imaging would be desirable include monitoring of physical therapy beyond the bedside or rehabilitation (Holper et al., 2010; Mihara et al., 2007), when social interactions between subjects are required, or when imaging children or infants (Hoshi and Chen, 2002; Mehnert et al., in press; Pastewski et al., 2012).
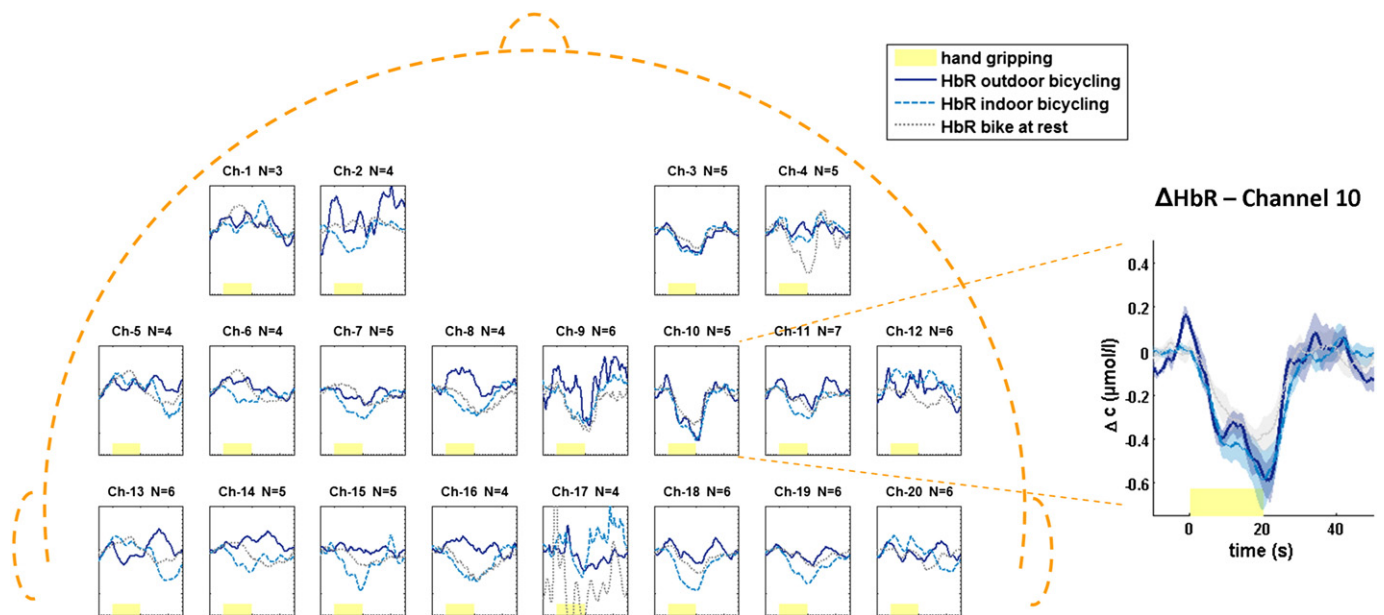

Fig. 5. Group averaged ΔHbR time courses for all channels and all three conditions: Labels on top indicate the channel number (e.g. Ch-1) and the overall number of subjects averaged in each condition of the corresponding channel. All subplots are scaled as shown in the enlarged channel 10 (insert right), which showed a significant HbR decrease 8–20 s after hand gripping onset in all three conditions. In the insert, the SEM is indicated in shaded colors. Yellow bars represent the hand-gripping period.

Conclusions and perspectives

The brain activation patterns measured in left hand gripping during bicycle riding demonstrate the feasibility of our compact wearable NIRS device for realistic studies in increasing ecological situations. To the best of our knowledge, this is the first demonstration of functional NIRS brain imaging during an outdoor activity in a real life environment. The task used in the present study investigates the detectability of a focal cerebral activation in response to a simple unilateral motor task in the presence of continuous background motor activity. While the task chosen is clearly experimental and serves methodological demonstration, the general scenario can be considered a starting point for the exploitation of ambulatory NIRS-monitoring in rehabilitation. Regarding gait, enhanced recruitment of premotor areas in subjects with gait impairment has been demonstrated (Mihara et al., 2007) and the contributions of areas relevant for motor control have been investigated during balance training in stroke victims (Fujimoto et al., 2014). The option of a fully portable instrument, as demonstrated in the present paper, may extend the options for dual tasks involving motor and more cognitive components. This may be of special interest because the interface between physical activity and cognitive function has become a hot topic not only in research in stroke patients (Chen et al., 2013) but also regarding successful aging.

Acknowledgments

References

Atsumori, H., Kiguchi, M., Obata, A., Sato, H., Katura, T., Utsugi, K., Funane, T., Maki, A., 2007. Development of a multi-channel, portable optical topography system. Conf. Proc. IEEE Eng. Med. Biol. Soc. 2007, 3362–3364.

Atsumori, H., Kiguchi, M., Obata, A., Sato, H., Katura, T., Funane, T., Maki, A., 2009. Development of wearable optical topography system for mapping the prefrontal cortex activation. Rev. Sci. Instrum. 80, 043704.

Atsumori, H., Kiguchi, M., Katura, T., Funane, T., Obata, A., Sato, H., Manaka, T., Iwamoto, M., Maki, A., Koizumi, H., Kubota, K., 2010. Noninvasive imaging of prefrontal activation during attention-demanding tasks performed while walking using a wearable optical topography system. J. Biomed. Opt. 15, 046002.

Boas, D.A., Dale, A.M., Franceschini, M.A., 2004. Diffuse optical imaging of brain activation: approaches to optimizing image sensitivity, resolution, and accuracy. Neuroimage 23 (Suppl. 1), S275–S288.

Bozkurt, A., Rosen, A., Rosen, H., Onaral, B., 2005. A portable near infrared spectroscopy system for bedside monitoring of newborn brain. Biomed. Eng. Online 4, 29.

Brett, M., Johnsrude, I.S., Owen, A.M., 2002. The problem of functional localization in the human brain. Nat. Rev. Neurosci. 3, 243–249.

Cannestra, A.F., Pouratian, N., Shomer, M.H., Toga, A.W., 1998. Refractory periods observed by intrinsic signal and fluorescent dye imaging. J. Neurophysiol. 80, 1522–1532.

Chen, C., Leys, D., Esquenazi, A., 2013. The interaction between neuropsychological and motor deficits in patients after stroke. Neurology 80, S27–S34.

Cooper, R.J., Gagnon, L., Goldenholz, D.M., Boas, D.A., Greve, D.N., 2012. The utility of near-infrared spectroscopy in the regression of low-frequency physiological noise from functional magnetic resonance imaging data. Neuroimage 59, 3128–3138.

Dehghani, H., White, B.R., Zeff, B.W., Tizzard, A., Culver, J.P., 2009. Depth sensitivity and image reconstruction analysis of dense imaging arrays for mapping brain function with diffuse optical tomography. Appl. Opt. 48, D137–D143.

Eggebrecht, A.T., White, B.R., Ferradal, S.L., Chen, C., Zhan, Y., Snyder, A.Z., Dehghani, H., Culver, J.P., 2012. A quantitative spatial comparison of high-density diffuse optical tomography and fMRI cortical mapping. Neuroimage 61, 1120–1128.

Essenpreis, M., Elwell, C.E., Cope, M., van der Zee, P., Arridge, S.R., Delpy, D.T., 1993. Spectral dependence of temporal point spread functions in human tissues. Appl. Opt. 32, 418–425.

Fazli, S., Mehnert, J., Steinbrink, J., Curio, G., Villringer, A., Muller, K.R., Blankertz, B., 2012. Enhanced performance by a hybrid NIRS-EEG brain computer interface. Neuroimage 59, 519–529.

Ferrari, M., Quaresima, V., 2012. A brief review on the history of human functional near-infrared spectroscopy (fNIRS) development and fields of application. Neuroimage 63, 921–935.

Franceschini, M.A., Fantini, S., Thompson, J.H., Culver, J.P., Boas, D.A., 2003. Hemodynamic evoked response of the sensorimotor cortex measured noninvasively with near-infrared optical imaging. Psychophysiology 40, 548–560.

Fujimoto, H., Mihara, M., Hattori, N., Hatakenaka, M., Kawano, T., Yagura, H., Miyai, I., Mochizuki, H., 2013. Cortical changes underlying balance recovery in patients with hemiplegic stroke. Neuroimage 85, 547–554.

Gevins, A., Chan, C.S., Sam-Vargas, L., 2012. Towards measuring brain function on groups of people in the real world. PLoS One 7, e44676.

Gregg, N.M., White, B.R., Zeff, B.W., Berger, A.J., Culver, J.P., 2010. Brain specificity of diffuse optical imaging: improvements from superficial signal regression and tomography. Front. Neuroenerg. 2.

Habermehl, C., Holtze, S., Steinbrink, J., Koch, S.P., Obrig, H., Mehnert, J., Schmitz, C.H., 2012a. Somatosensory activation of two fingers can be discriminated with ultrahigh-density diffuse optical tomography. Neuroimage 59, 3201–3211.

Habermehl, C., Schmitz, C.H., Steinbrink, J., 2012b. Contrast enhanced high-resolution diffuse optical tomography of the human brain using ICG. Opt. Express 19, 18636–18644.

Habermehl, C., Schmitz, C., Koch, S.P., Mehnert, J., Steinbrink, J., 2012c. Investigating hemodynamics in scalp and brain using high-resolution diffuse optical tomography in humans. Biomedical Optics, OSA Technical Digest (Optical Society of America, 2012) paper BSu2A.2.

Hoge, R.D., Franceschini, M.A., Covolan, R.J., Huppert, T., Mandeville, J.B., Boas, D.A., 2005. Simultaneous recording of task-induced changes in blood oxygenation, volume, and flow using diffuse optical imaging and arterial spin-labeling MRI. Neuroimage 25, 701–707.

Holper, L., Muehlemann, T., Scholkmann, F., Eng, K., Kiper, D., Wolf, M., 2010. Testing the potential of a virtual reality neurorehabilitation system during performance of observation, imagery and imitation of motor actions recorded by wireless functional near-infrared spectroscopy (fNIRS). J. Neuroeng. Rehabil. 7, 57.

Holtzer, R., Mahoney, J.R., Izzetoglu, M., Izzetoglu, K., Onaral, B., Verghese, J., 2011. fNIRS study of walking and walking while talking in young and old individuals. J. Gerontol. A Biol. Sci. Med. Sci. 66, 879–887.

Hoshi, Y., Chen, S.J., 2002. Regional cerebral blood flow changes associated with emotions in children. Pediatr. Neurol. 27, 275–281.

Huppert, T.J., Hoge, R.D., Diamond, S.G., Franceschini, M.A., Boas, D.A., 2006. A temporal comparison of BOLD, ASL, and NIRS hemodynamic responses to motor stimuli in adult humans. Neuroimage 29, 368–382.

Huppert, T.J., Franceschini, M.A., Boas, D.A., 2009. Noninvasive imaging of cerebral activation with diffuse optical tomography, In: Frostig, R.D. (Ed.), In Vivo Optical Imaging of Brain Function, 2nd edition. CRC Press, Boca Raton (FL).

Kiguchi, M., Atsumori, H., Fukasaku, I., Kumagai, Y., Funane, T., Maki, A., Kasai, Y., Ninomiya, A., 2012. Note: wearable near-infrared spectroscopy imager for haired region. Rev. Sci. Instrum. 83, 056101.

Kirilina, E., Jelzow, A., Heine, A., Niessing, M., Wabnitz, H., Bruhl, R., Ittermann, B., Jacobs, A.M., Tachtsidis, I., 2012. The physiological origin of task-evoked systemic artefacts in functional near infrared spectroscopy. Neuroimage 61, 70–81.

Kleinschmidt, A., Obrig, H., Requardt, M., Merboldt, K.D., Dirnagl, U., Villringer, A., Frahm, J., 1996. Simultaneous recording of cerebral blood oxygenation changes during human brain activation by magnetic resonance imaging and near-infrared spectroscopy. J. Cereb. Blood Flow Metab. 16, 817–826.

Koch, S.P., Habermehl, C., Mehnert, J., Schmitz, C.H., Holtze, S., Villringer, A., Steinbrink, J., Obrig, H., 2012. High-resolution optical functional mapping of the human somatosensory cortex. Front. Neuroenerg. 2, 12.

Kocsis, L., Herman, P., Eke, A., 2006. The modified Beer–Lambert law revisited. Phys. Med. Biol. 51, N91–N98.

Koenraadt, K.L., Duysens, J., Smeenk, M., Keijsers, N.L., 2012. Multi-channel NIRS of the primary motor cortex to discriminate hand from foot activity. J. Neural Eng. 9, 046010.

Krueger, A., Koch, S.P., Mehnert, J., Habermehl, C., Piper, S., Steinbrink, J., Obrig, H., Schmitz, C.H., 2012. Imaging of Motor Activity in Freely Moving Subjects Using a Wearable NIRS Imaging System. Biomedical Optics, OSA Technical Digest (Optical Society of America, 2012), p. BM4A.3.

Kurz, M.J., Wilson, T.W., Arpin, D.J., 2012. Stride-time variability and sensorimotor cortical activation during walking. Neuroimage 59, 1602–1607.

Lareau, E., Lesage, F., Pouliot, P., Nguyen, D., Le Lan, J., Sawan, M., 2011. Multichannel wearable system dedicated for simultaneous electroencephalographynear-infrared spectroscopy real-time data acquisitions. J. Biomed. Opt. 16, 096014.

Leff, D.R., Orihuela-Espina, F., Elwell, C.E., Athanasiou, T., Delpy, D.T., Darzi, A.W., Yang, G.Z., 2011. Assessment of the cerebral cortex during motor task behaviours in adults: a systematic review of functional near infrared spectroscopy (fNIRS) studies. Neuroimage 54, 2922–2936.

Mehagnoul-Schipper, D.J., van der Kallen, B.F., Colier, W.N., van der Sluijs, M.C., van Erning, L.J., Thijssen, H.O., Oeseburg, B., Hoefnagels, W.H., Jansen, R.W., 2002. Simultaneous measurements of cerebral oxygenation changes during brain activation by near-infrared spectroscopy and functional magnetic resonance imaging in healthy young and elderly subjects. Hum. Brain Mapp. 16, 14–23.

Mehnert, J., Akhrif, A., Telkemeyer, S., Rossi, S., Schmitz, C.H., Steinbrink, J., Wartenburger, I., Obrig, H., Neufang, S., 2013. Developmental changes in brain activation and functional connectivity during response inhibition in the early childhood brain. Brain Dev. http://dx.doi.org/10.1016/j.braindev.2012.11.006 (in press).

Mihara, M., Miyai, I., Hatakenaka, M., Kubota, K., Sakoda, S., 2007. Sustained prefrontal activation during ataxic gait: a compensatory mechanism for ataxic stroke? Neuroimage 37, 1338–1345.

Moosmann, M., Ritter, P., Krastel, I., Brink, A., Thees, S., Blankenburg, F., Taskin, B., Obrig, H., Villringer, A., 2003. Correlates of alpha rhythm in functional magnetic resonance imaging and near infrared spectroscopy. Neuroimage 20, 145–158.

Muehlemann, T., Haensse, D., Wolf, M., 2008. Wireless miniaturized in-vivo near infrared imaging. Opt. Express 16, 10323–10330.

Muehlemann, T., Holper, L., Wenzel, J., Wittkowski, M., Wolf, M., 2013. The effect of sudden depressurization on pilots at cruising altitude. Adv. Exp. Med. Biol. 765, 177–183.

Obrig, H., Villringer, A., 2003. Beyond the visible—imaging the human brain with light. J. Cereb. Blood Flow Metab. 23, 1–18.

Obrig, H., Hirth, C., Junge-Hulsing, J.G., Doge, C., Wenzel, R., Wolf, T., Dirnagl, U., Villringer, A., 1997. Length of resting period between stimulation cycles modulates hemodynamic response to a motor stimulus. Adv. Exp. Med. Biol. 411, 471–480.

Obrig, H., Neufang, M., Wenzel, R., Kohl, M., Steinbrink, J., Einhaupl, K., Villringer, A., 2000. Spontaneous low frequency oscillations of cerebral hemodynamics and metabolism in human adults. Neuroimage 12, 623–639.

Obrig, H., Israel, H., Kohl-Bareis, M., Uludag, K., Wenzel, R., Muller, B., Arnold, G., Villringer, A., 2002. Habituation of the visually evoked potential and its vascular response: implications for neurovascular coupling in the healthy adult. Neuroimage 17, 1–18.

Pastewski, M., Kleiser, S., Metz, A., Wolf, M., 2012. A wireless, self-calibrating sensor for fNIRS studies in preterm infants. Functional Near Infrared Spectroscopy Conference Oct. 26th–28th 2012 London.

Prahl, Scott, O.M.L.C., 2006. Tabulated Molar Extinction Coefficient for Hemoglobin in Water.

Saager, R., Berger, A., 2008. Measurement of layer-like hemodynamic trends in scalp and cortex: implications for physiological baseline suppression in functional near-infrared spectroscopy. J. Biomed. Opt. 13, 034017.

Sagara, K., Kido, K., Ozawa, K., 2009. Portable single-channel NIRS-based BMI system for motor disabilities' communication tools. Conf. Proc. IEEE Eng. Med. Biol. Soc. 2009, 602–605.

Sato, H., Kiguchi, M., Kawaguchi, F., Maki, A., 2004. Practicality of wavelength selection to improve signal-to-noise ratio in near-infrared spectroscopy. Neuroimage 21, 1554–1562.

Schmitz, C.H., Loecker, M., Lasker, J.M., Hielscher, A.H., Barbour, R.L., 2002. Instrumentation for fast functional optical tomography. Rev. Sci. Instrum. 73.

Schmitz, C.H., Klemer, D.P., Hardin, R., Katz, M.S., Pei, Y., Graber, H.L., Levin, M.B., Levina, R.D., Franco, N.A., Solomon, W.B., Barbour, R.L., 2005. Design and implementation of dynamic near-infrared optical tomographic imaging instrumentation for simultaneous dual-breast measurements. Appl. Opt. 44, 2140–2153.

Schneider, P., Piper, S., Schmitz, C.H., Schreiter, N.F., Volkwein, N., Ludemann, L., Malzahn, U., Poellinger, A., 2011. Fast 3D near-infrared breast imaging using indocyanine green for detection and characterization of breast lesions. Rofo 183, 956–963.

Shalinsky, M.H., Kovelman, I., Berens, M.S., Petitto, L.A., 2009. Exploring cognitive functions in babies, children & adults with near infrared spectroscopy. J. Vis. Exp. 29, 1268. http://dx.doi.org/10.3791/1268.

Steinbrink, J., Villringer, A., Kempf, F., Haux, D., Boden, S., Obrig, H., 2006. Illuminating the BOLD signal: combined fMRI–fNIRS studies. Magn. Reson. Imaging 24, 495–505.

Steinkellner, O., Gruber, C., Wabnitz, H., Jelzow, A., Steinbrink, J., Fiebach, J.B., Macdonald, R., Obrig, H., 2010. Optical bedside monitoring of cerebral perfusion: technological and methodological advances applied in a study on acute ischemic stroke. J. Biomed. Opt. 15, 061708.

Strangman, G., Culver, J.P., Thompson, J.H., Boas, D.A., 2002. A quantitative comparison of simultaneous BOLD fMRI and NIRS recordings during functional brain activation. Neuroimage 17, 719–731.

Strangman, G., Franceschini, M.A., Boas, D.A., 2003. Factors affecting the accuracy of near-infrared spectroscopy concentration calculations for focal changes in oxygenation parameters. Neuroimage 18, 865–879.

Suzuki, M., Miyai, I., Ono, T., Oda, I., Konishi, I., Kochiyama, T., Kubota, K., 2004. Prefrontal and premotor cortices are involved in adapting walking and running speed on the treadmill: an optical imaging study. Neuroimage 23, 1020–1026.

Suzuki, M., Miyai, I., Ono, T., Kubota, K., 2008. Activities in the frontal cortex and gait performance are modulated by preparation. An fNIRS study. Neuroimage 39, 600–607.

Tobias, J.D., 2006. Cerebral oxygenation monitoring: near-infrared spectroscopy. Expert Rev. Med. Devices 3, 235–243.

Toet, M.C., Lemmers, P.M., 2009. Brain monitoring in neonates. Early Hum. Dev. 85, 77–84.

Vaithianathan, T., 2004. Design of a portable near infrared system for topographic imaging of the brain in babies. Rev. Sci. Instrum. 75, 3276–3283.

Villringer, A., Chance, B., 1997. Non-invasive optical spectroscopy and imaging of human brain function. Trends Neurosci. 20, 435–442.

Wallois, F., Mahmoudzadeh, M., Patil, A., Grebe, R., 2012. Usefulness of simultaneous EEG-NIRS recording in language studies. Brain Lang. 121, 110–123.

White, B.R., Culver, J.P., 2010. Quantitative evaluation of high-density diffuse optical tomography: in vivo resolution and mapping performance. J. Biomed. Opt. 15, 026006.

Yurtsever, G., Bozkurt, A., Kepics, F., Pourrezaei, K., Devaraj, A., 2003. Pocket PC based wireless continuous wave near infrared spectroscopy system for functional imaging of human brain Engineering in Medicine and Biology Society, 2003. Proceedings of the 25th Annual International Conference of the IEEE.

Zhang, Y., Brooks, D.H., Franceschini, M.A., Boas, D.A., 2005. Eigenvector-based spatial filtering for reduction of physiological interference in diffuse optical imaging. J. Biomed. Opt. 10, 11014.

Zhang, Q., Strangman, G.E., Ganis, G., 2009. Adaptive filtering to reduce global interference in non-invasive NIRS measures of brain activation: how well and when does it work? Neuroimage 45, 788–794.